http://dx.doi.org/10.21611/qirt.2002.038

# Detection of defects of foil sensors applied in the automotive industry by means of active ir thermography

by C. Gruss [1], J. Gibkes [2]

[(1)] *International Electronics & Engineering, Zone Industrielle, 6468 Echternach Luxembourg*
*Tel. +352-7289896331, Fax +352-7289896309, e-mail: Christian.gruss@iee.lu*
[(2)] *Ruhr-University Bochum, Exp. Phys. III, D-44780 Bochum, germany*

**Abstract:**

Examples of industrial application of the active Infrared Thermography are presented here. IEE Luxembourg produces foil sensors which are applied in car seats in order to detect the presence of a passenger or alternatively of a child seat. This information is supplied to the airbag electronics which thus knows whether it should deploy or not in the case of accident. The sensors are made of two plastic foils with printed electrical circuits. The input of electrical current produces heat sources due to the electrical resistivity of the lines, especially at the position of local inhomogeneities, which can be detected by this technique.

## 1. Introduction

According to Vavilov [1], the use of infrared techniques for the control of electronic devices in the industry started in the 60's. Recent applications in the semi conductor field have been described for example by Wiecek and al. [2]. IR imaging has been used, for example by Yiqian [3], to control printed circuits. In our case we have applied active IR thermography to control the integrity of printed silver circuits. After printing the electrically conducting lines on the separate sensor foil, the global electrical resistance is measured first. If there is an interruption of the conducting line, the resistance increases dramatically. If the line is not totally interrupted, the resistance increase is not detectable since the electrical test relies on a global measurement. A conducting line of reduced size, however, can make problems in the future, when due to mechanical aging of the sensor the line will be cut completely. By injecting electrical current in the printed line and by observing the sensor with an IR camera, effects of anomalous heating can be observed in an eventually future defect zone. The method is non-destructive and non-intrusive for the fabrication process, since the electrical contacts with the printed circuit already exist due to the resistance test used so far. The second application is the possibility to detect defects in complete sensors without damaging or cutting them.

In the following we present some theoretical considerations to explain the inspection technique and then some applications are shown.

## 2. Theory

A sensor is placed on a flat table in the Field of View (FOV) of an IR camera. The electrodes of the sensor to be tested are connected to a current generator. First an IR image is taken from the sensor without current which will be used as reference image in order to eliminate parasitic reflection. Then, when the current is switched on, the IR camera is activated. From the obtained image, the reference image is subtracted, so that only the thermal response to the heating pulse due to the current input remains.

The electrical energy is transformed by the Joule effect in thermal energy according to the law Power $P = RI^2$, with R the electrical resistance and I the current. In a first approximation (i.e. by neglecting heat diffusion), the temperature increase $\Delta T$ at the time $\Delta t$ is given by:

http://dx.doi.org/10.21611/qirt.2002.038

$$\Delta T = P\,\Delta t / C_L \quad (1)$$

with $C_L$ the heat capacity of the heated line. We can write $C_L = S \times L \times C$, with S the cross section of the conducting line, L the considered length of the conducting line and C the heat capacity per volume unit. With the electrical resistance $R = \rho_e\, L/S$, we thus obtain:

$$\Delta T = (I/S)^2\,\Delta t\,\rho_e/C \quad (2)$$

Thus at a given time $\Delta t$ and if we consider the material parameters $\rho_e$ and C as constants, the temperature variation is related to the variation of the inverse quadratic of the line cross section. Local non-homogeneity of the conducting line corresponding to a reduced cross section can lead to an increased temperature at the position of the defect.

Owing to the design, however, the cross section can also change locally. Thus, in the analysis of the temperature increase, the design-related temperature variations also have to be taken into account.

In this short qualitative discussion, the effects of heat propagation are neglected, which means that the result is true only for the first seconds of heating. After a certain time, correction factors have to be considered.

## 3. Results

The first use of the active IR thermography is to control the integrity of the sensor just after being printed, i.e. when the printed circuit is not yet covered by the protecting second plastic foil. Figure 1 shows the image of such a print, taken 1s after the beginning of the current input of 340 mA, and Figure 2 shows a detail of the temperature profile along the printed silver line. One can clearly identify the local temperature increase due to the reduced thickness: The maximum temperature is 26,1°C, the ambient temperature measured on the non heated silver line is about 21°C, and the normal heated silver line has got a temperature of 24,5°C. From equation (2) one can determine the ratio of the cross sections of the normal silver line and of the defect line with the reduced cross section:

$$\Delta T_{defect}/\Delta T_{normal} = (S_{normal}/S_{defect})^2 = 5{,}5/3{,}5 = 1{,}57 \quad (3)$$

Thus we can find an effective cross section deficit of about 21% in the region where the defect is localized. The optically measured defect shows a deficit of about 50% of the cross section. To explain this difference one has to consider that the spatial resolution of the camera used here (1 mm) is larger than the printed line (0.5 mm) and that thus a convolution effect has to be taken into account. Nevertheless the method is sufficiently sensitive to localize the defects and to estimate their order of magnitude.

A second possibility to use the active IR Thermography, is to analyse complete sensors after mechanical tests in order to verify if a printed line has been damaged without destroying the foil sensor itself. Figure 3 shows the IR camera image of a sensor after a mechanical test, taken 20s after switching on a current of 0,2 A. Various spots with higher temperatures are observed on the complete sensor, which in Figure 4 are shown with an improved temperature resolution.

The time-dependent temperature increase has been measured for the hot spots of Figure 4. Figure 5 presents the resulting curves for the spots 01 to 07, with spot 07 as reference position, where no heating occurs and the temperature remains constant at about 22,5°C. We can see that for time intervals smaller than $\Delta t$ = 2s, the temperature variation is relatively linear with time. Thus, after this time interval $\Delta t$ the assumption of negligible heat diffusion used to establish equ. (1) and (2) is no longer correct and part of the differences between the thermally effective cross section according to eqn. (3) and the optically measured cross section may be explained.

For the spots 01 to 06, the printed silver line has normally a lateral thickness of 2 mm. The spots 03 and 06, taken in the middle of the electrodes where no overheating exists,

http://dx.doi.org/10.21611/qirt.2002.038

show maximum temperatures of 24,5°C and 23,9°C, respectively, with a temperature increase between about 2,0°C and 1,4°C.

In contrast, the spots 01 and 04 are located on two positions of the electrode where the temperatures reach maximum values 35°C and 37,9°C, with temperature increases of 12,5°C and 15,4°C. Thus, the ratios of the temperature increases are $\Delta T_{spot\ 01}/\Delta T_{spot\ 03} = 6,3$ and $\Delta T_{spot\ 04}/\Delta T_{spot\ 06} = 11$. According to equ.(3) we have $(S_{spot\ 03}/S_{spot\ 01})^2 = \Delta T_{spot\ 01}/\Delta T_{spot\ 03}$. Assuming that the thickness of the printed layer is constant, we then get for the lateral widths of the printed line the ratios $w_{spot\ 03}/w_{spot\ 01} = 2.5$ and $w_{spot\ 06}/w_{spot\ 04} = 3;3$. In comparison with the spots 04 and 01, the spots 02 and 05 represent secondary maxima. This analysis clearly shows the defects in the region of the spots 01, 02, 04 and 05, where the sensor had been submitted to mechanical strain.

Figure 6 shows the time-dependent temperatures measured for the spots 24 to 31. The spots 29 and 30 are from regions where the silver line has got a thickness of only 0,5 mm, and where maximum temperatures of 30,6°C and 28,2°C have been measured, corresponding to an increase of 8,1°C and 5,7°C, respectively.

Spot 25 and 31 are located where the lateral width of the silver line is about 2 mm: maximum temperatures of only 24,9°C and 24,1°C are measured, which are in agreement with the values of spot 3 and spot 6, which also have a lateral width of 2 mm.

The spots 24 and 26 are also localized on a 2 mm thick silver line, however, here the maximum temperatures are 27,3°C and 27,9°C, which means temperature increases of 4,8°C and 5,4°C are observed, instead of 2,4°C or 1,6°C as observed for the spots 25 and 31. Thus, the equivalent lateral width should be between 1,3 mm and 1,2 mm. Since there is no mechanical damage, we are sure that these defects are defects of printing.

Spot 27 and 28 are from a region where two lines of 0,5 mm width exist, however with a distance of only 2 mm between them. The optothermal resolution is not high enough to separate the two lines, instead larger temperature increases of 15,5°C and 14,9°C are observed, in comparison with the normal temperature increase of a single line, which is about 6°C to 8°C. In fact, maximum temperatures of 38°C and 37,4°C have been measured. Thus, the temperature increase is a factor of 2 larger than for a single line, and we can assume that twice the energy has been deposited in comparison with a single line.

Figure 7 shows the time-dependent temperature increases of the spots 08, 09, 10, 11, 13 17, 18 and 19. All spots are on a double silver line with a width of 0,5 mm of each single line and a 1,5 mm distance between the two single lines. The spots 08, 10, 11 and 13 have got maximum temperatures of 48,7°C, 38,7°C, 42,9°C and 35,7°C, respectively. We see that spot 11 and especially spot 8 have got a larger temperature than spot 10 and 13. Observing additionally that the spots 09, 17, 18 and 19 have got maximum temperatures of about 35°C, we can conclude that the spots 13, 11, and especially 08 have got defects. In fact with a 35°C maximum temperature, we have a 12,5°C temperature increase, which is approximately twice the temperature increase as observed for spot 29 and 30 which have got a width of 0,5 mm. In contrast, spot 08 has got a temperature increase of 26.2°C, which is a factor of 2 larger than that of the other spots of the double line composed by two single lines each of 0.5 mm width.

Figure 8 confirms the measurements presented in Figure 7. Nearly all spots have got a maximum temperature of about 35°C, with exception of the spot 12, which is symmetrical to spot 8 with its maximum temperature of 43,3°C and a temperature increase of 22,9°C. Thus the calculated width of spot 12 is about 25% smaller than that of the other spots. From the fact that the defect spots 8 and 12 are found in a symmetrical position one can conclude that these defects are systematical ones, probably related to a mechanically induced effect.

## 4. Conclusion

The application of active IR imaging has been tested for electronic foil sensors consisting of printed conducting lines, by using electrical heating as source of excitation.

http://dx.doi.org/10.21611/qirt.2002.038

Local non-homogeneities have successfully been detected, which are due to failures in the production process or induced by mechanical tests simulating normal mechanical aging and wear processes. The design of such foil sensors can also be improved by mechanical tests and simultaneous or subsequent active IR imaging.

The present study which only relies on empirical tests and the qualitative discussion of the IR images has given reliable and sufficient information to implement such tests under the conditions of industrial production. For an improved quantitative analysis, which may be useful for sensor design studies, a complete theoretical study may be necessary, taking into account the convolution effects induced by the limited lateral resolution of the detector and the effects of 3-D heat propagation, as done in [4] for the case of the modulated IR technique for the determination of layer thickness.

## REFERENCES

[1] VAVILOV, V., “Thermal non destructive testing: short history and state-of-art”, QIRT 92, Edition Européennes Thermique et Industrie, Paris, France, 1992, pp 179-194.

[2] WIECEK, B., GRECKI, M. and PACHOLIK, J., “Thermal measurements of power semi conductor devices using thermographic system”, QIRT 92, Edition Européennes Thermique et Industrie, Paris, France, 1992, pp 291-295.

[3] YIQIAN, W. “Thermal wave imaging: Flying-spot camera”, PhD thesis, The Wayne State University, Detroit, Michigan, USA, 1992.

[4] GRUSS, C. “Building of a photothermal apparatus using thermal waves for the determination of layer thickness in industrial environment“, Grant report Stiftung Industrieforschung, Köln, Germany, Aug. 1998.

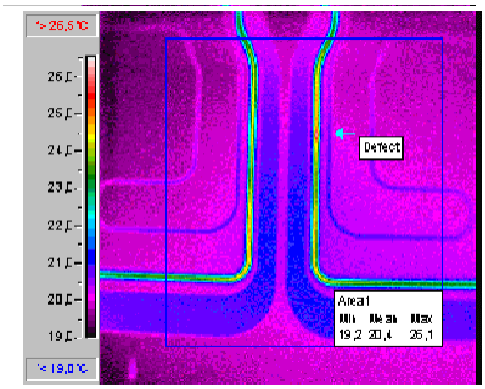


***Fig. 1**. IR image of a sensor foil after 340 mA current input during 1s.*

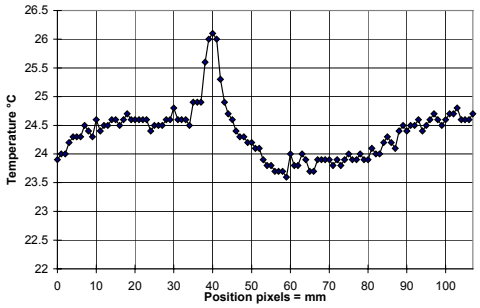


***Fig. 2.** Temperature profile along the conductive silver line of Figure 1.*

http://dx.doi.org/10.21611/qirt.2002.038

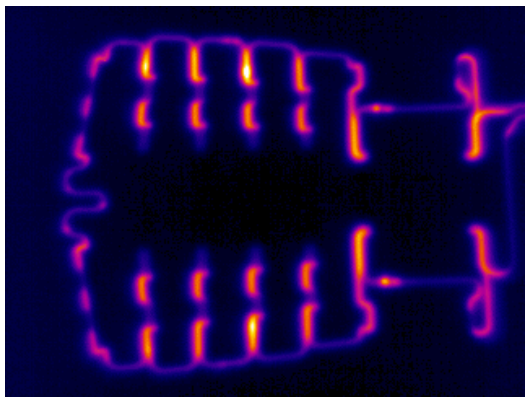

***Fig. 3.*** *IR image of the complete sensor, 20s after switching on a current of 0.2 A.*

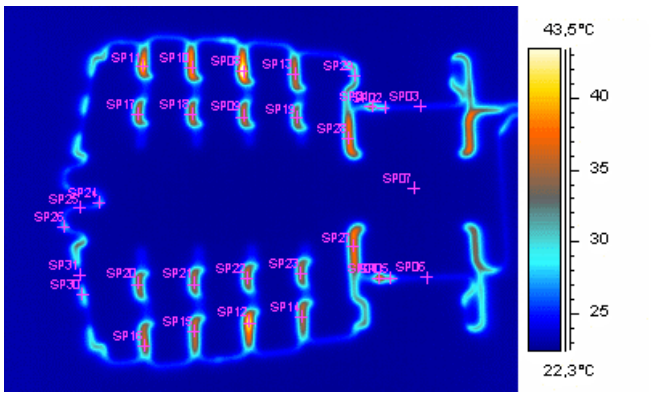


***Fig. 4.*** *IR image of the complete sensor with improved temperature resolution, taken 20s after switching on a 0.2 A current.*

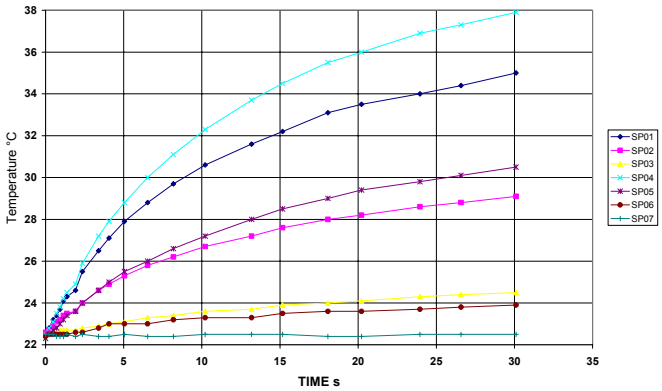


***Fig. 5.*** *Time dependent temperature increase of spots 01 to 07*

http://dx.doi.org/10.21611/qirt.2002.038

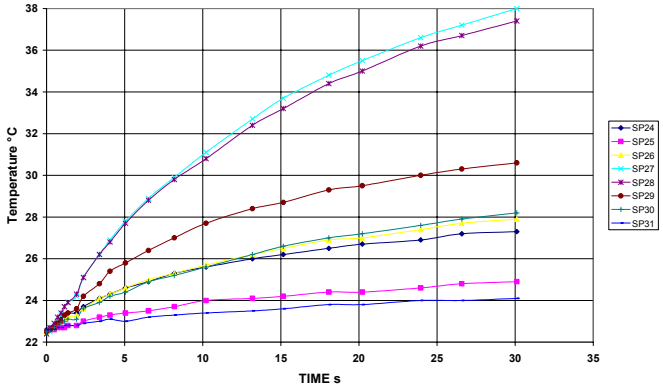


***Fig. 6.*** *Time dependent temperature increase of spots 24 to 31*

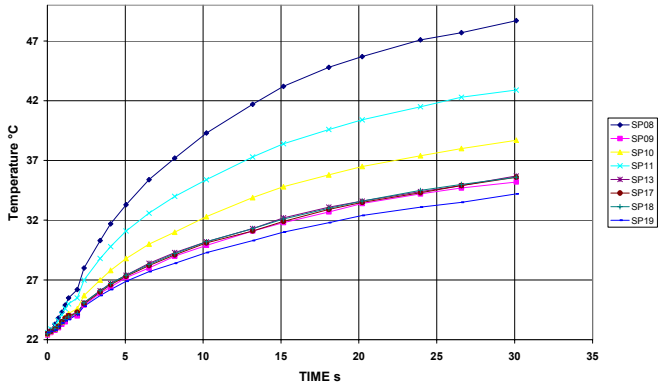


***Fig. 7.*** *Time dependent temperature increase of spots 08, 09, 10, 11, 13 17, 18 and 19.*

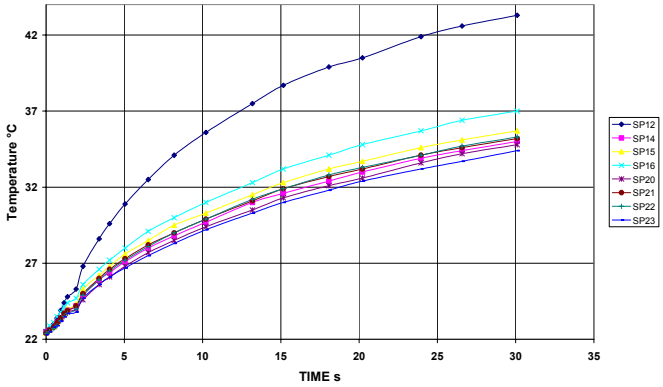


***Fig. 8.*** *Time dependent temperature increase of spots 12, 14, 15, 16, 20 21, 22 and 23*